SUPPLEMENTAL INFORMATION

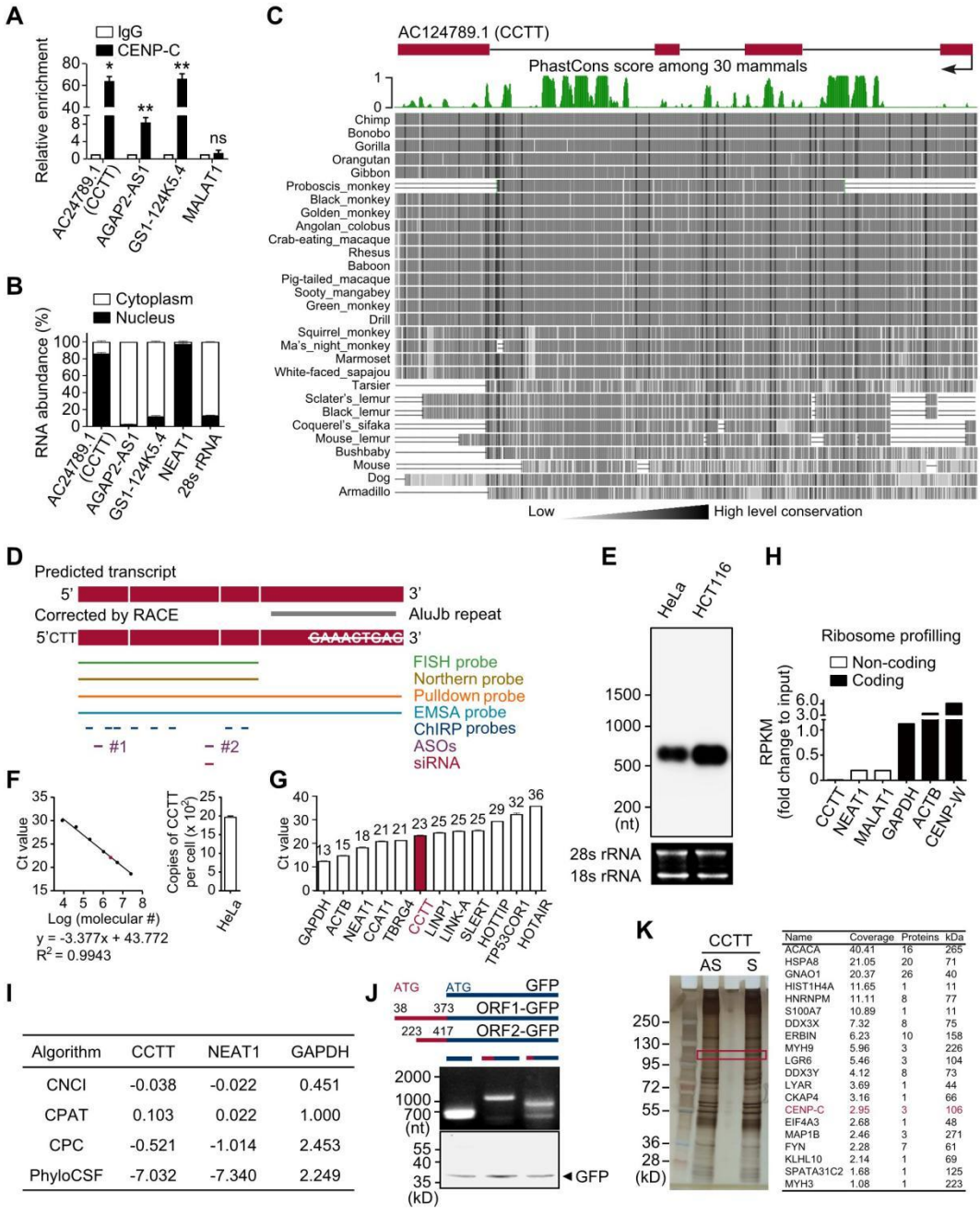

Figure S1. Screening LncRNAs Interacting with CENP-C, Related to Figure 1

(A) CENP-C RIP followed by qPCR analysis of AC24789.1 (CCTT), AGAP2-AS1, and GS1-124K5.4 in HeLa cells. MALAT1 was used as a

negative control. *p < 0.05; **p < 0.01; ns, no significant difference (mean ± SD, n = 3 per group).

(B) Percentage of CCTT, AGAP2-AS1, and GS1-124K5.4 expression in cytoplasmic and nuclear fractions of HeLa cells by qRT-PCR analysis. The nucleus-enriched NEAT1 and cytoplasm-enriched 28s rRNA were used as controls (mean ± SD, n = 3 per group).

(C) Conservation analysis of CCTT in 30 mammals.

(D) Diagram of the predicted CCTT transcript from UCSC Genome Browser tracks and accurate CCTT sequences corrected by 5' and 3' RACE which has 3 extra nucleotides (CTT) at the 5' end and misses 9 nucleotides (GAAACTGAG) at the 3' end compared to the annotated version, as well as the probes, ASOs, and siRNAs used in this study.

(E) Northern blot analysis of CCTT in HeLa and HCT116 cells using a probe against the Alu-deleted CCTT. Agarose gel showed comparable amount of total RNA.

(F) The copy number of CCTT per cell in HeLa cells. Left, the linear relationship between the log CCTT copy number and its CT value by qRT-PCR. Black dots represent known copies of CCTT from a plasmid DNA containing CCTT sequences and the red dot represents CCTT copies in HeLa cells. Right, the average copies of CCTT per cell (mean ± SD, n = 3 per group).

(G) The relative abundance of CCTT (red) in HeLa cells. The Ct value of each RNA was shown.

(H) Ratio of RPKM ribosome profiling relative to input RPKM in HeLa cells.

(I) Scores of CCTT, GAPDH (mRNA), and NEAT1 (lncRNA) determined by

CNCI, CPAT, CPC, and PhyloCSF algorithms.

(J) *In vitro* translation assay of the predicted CCTT ORFs (ORF1: 38-373 nt and ORF2: 222-417 nt). HeLa cells expressing the GFP-tagged CCTT ORFs, followed by western blot analysis of GFP. RT-PCR showed corresponding RNA.

(K) RNA pulldown with biotinylated sense or antisense CCTT from A549 cell lysates followed by mass spectrometry (MS) analysis. NuPAGE Bis-Tris gel picture (left) and MS analysis result (right) showed 20 CCTT-interacting candidate proteins including CENP-C. The band highlighted in red box contains CENP-C.

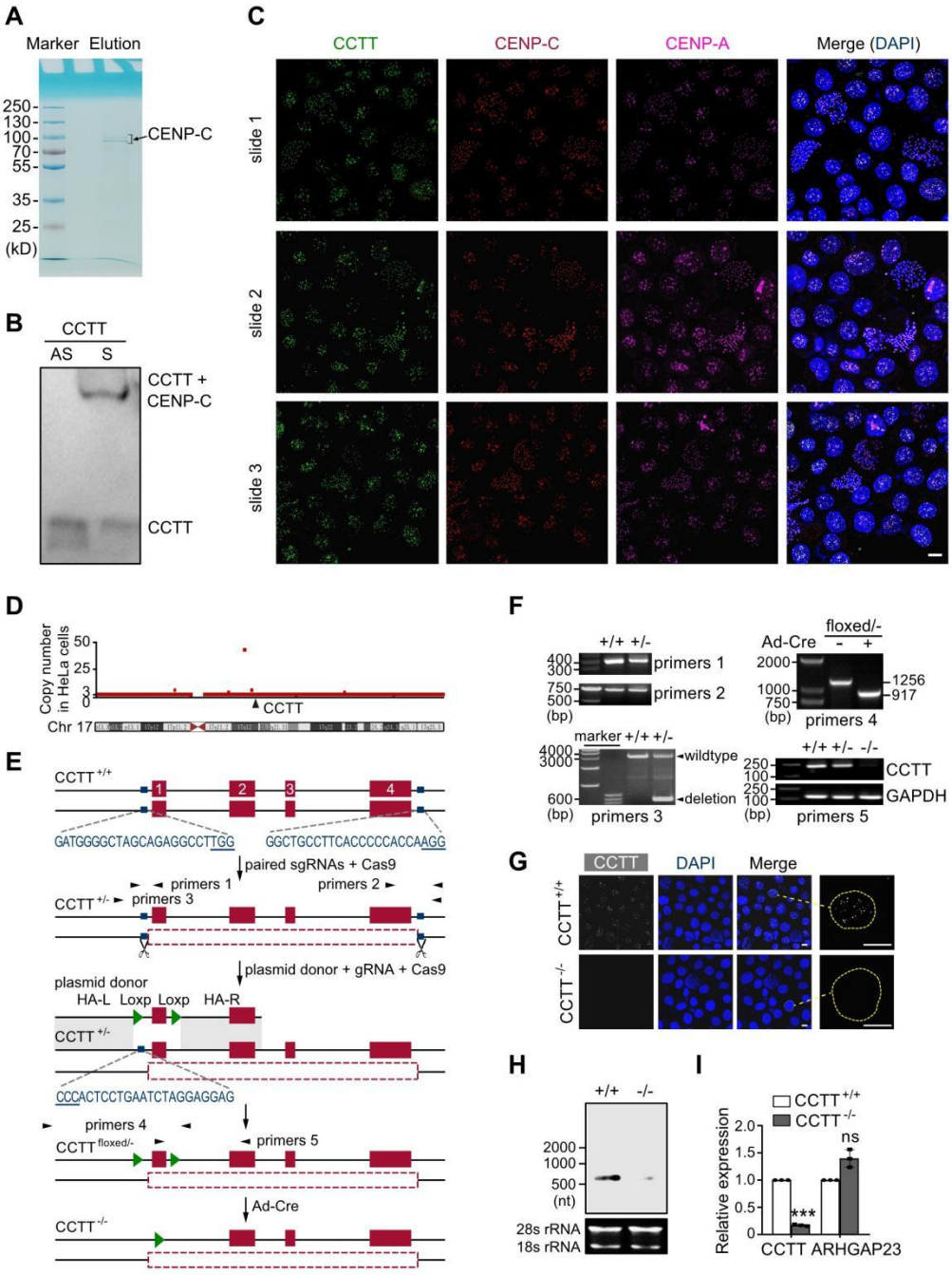

41 **Figure S2. CCTT colocalizes with CENP-C and Identification of**

42 **Conditional Knockout of CCTT, Related to Figures 1 and 2**

43 (A) His-tagged CENP-C was solved by 10% Tris-Glycine gel (SDS-PAGE) and

44 visualized using Coomassie Brilliant Blue Staining.

45 (B) EMSA assay of CCTT specifically interacted with CENP-C. EMSA imaging

with 0.7 pmol biotinylated sense or antisense CCTT binding to 2.5 μM purified recombinant CENP-C proteins.

(C) CCTT FISH (green), CENP-C (red) and CENP-A (pink) IF analyses of HeLa cells of three different slides are shown. Scale bars, 10 μm.

(D) The copy number of CCTT locus in HeLa cells. Most genes encoded by Chr. 17 have 3 copied as specifically indicated at the y-axis. The CCTT locus is labeled with a arrowhead.

(E) Schematic of the strategy for generating conditional CCTT knockout in HeLa cells stably expressing Cas9. The gRNA-coding sequences are blue with the protospacer-adjacent motif (PAM) sequences underlined. In the donor sequences, two LoxP sites flanking CCTT exon 1 are indicated as triangles. Primers for PCR genotyping are 1-4, while primers for RT-PCR are 5.

(F) Left: PCR analysis with primers 1, 2, and 3 to screen $CCTT^{+/-}$ cells. Products of primers 1 (391 bp) and 2 (715 bp) are specific for the wildtype allele and products of primers 3 are specific for the CCTT full-length deletion allele (3164 bp for wildtype allele and ~558 bp for deletion allele, showed by black arrow). Right top: PCR analysis with primers 4 in $CCTT^{floxed/-}$ cells after adenovirus-Cre (Ad-Cre) treatment. Right bottom: RT-PCR analysis with primers 5 for CCTT expression in $CCTT^{+/+}$, $CCTT^{+/-}$, and $CCTT^{-/-}$ cells.

(G) CCTT FISH (white) analysis of $CCTT^{+/+}$ and $CCTT^{-/-}$ cells. The right panel is the enlarged view of one selected cell. Scale bars, 10 μm.

(H) Northern blot analysis of CCTT expression in $CCTT^{+/+}$ and $CCTT^{-/-}$ cells using a probe against the Alu-deleted CCTT. Agarose gel shown bottom

indicates comparable amounts of total RNA.

(I) *ARHG*AP23 expression was unchanged in CCTT$^{-/-}$ cells. qRT-PCR analysis of CCTT and ARHGAP23 in CCTT$^{+/+}$ and CCTT$^{-/-}$ cells. ***p < 0.001; ns, no significant difference (mean ± SD, n = 3 per group).

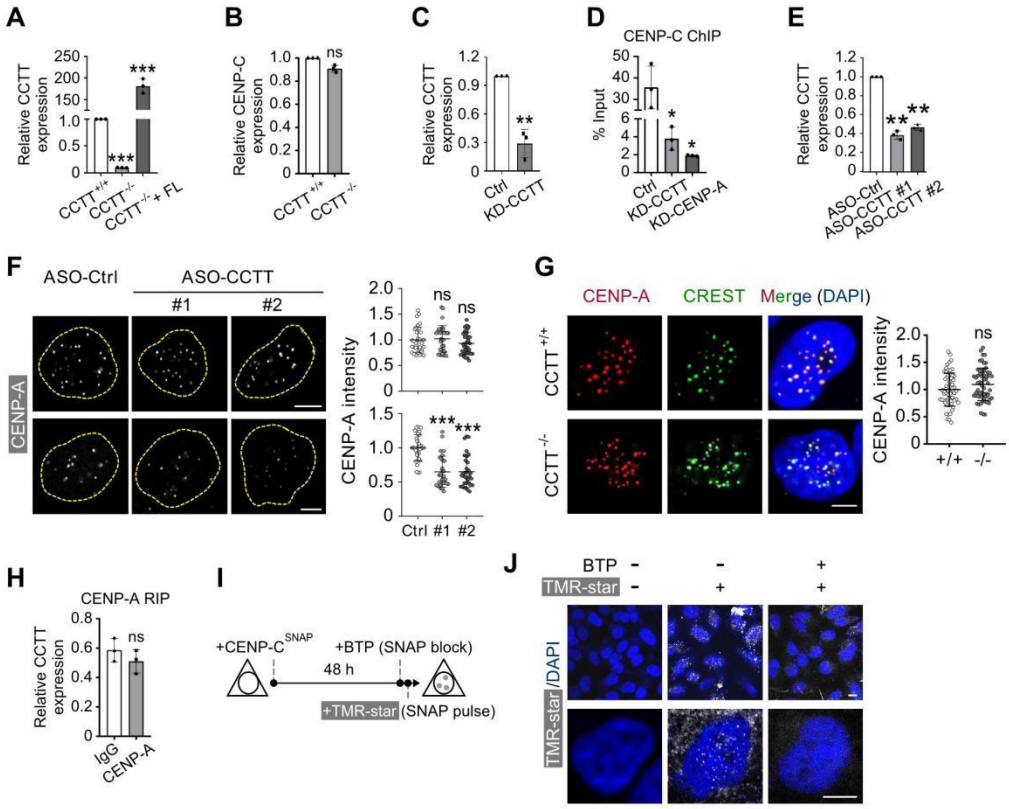

Figure S3. CCTT Does Not Affect Total CENP-C Level and Its Maintenance, as well as CENP-A at Centromeres, Related to Figure 2

(A) Re-expression of CCTT in CCTT$^{-/-}$ cells. Quantification of CCTT level in HeLa cells by qRT-PCR. ***p < 0.001 (mean ± SD, n = 3 per group).

(B) qRT-PCR analysis of CENP-C in CCTT$^{+/+}$ and CCTT$^{-/-}$ HeLa cells. ns, no significant difference (mean ± SD, n = 3 per group).

(C) CCTT knockdown (KD-CCTT) by siRNA treatment for 48 hours in HeLa cells. Quantification of CCTT level by qRT-PCR. **p < 0.01 (mean ± SD, n = 3 per group).

(D) CCTT knockdown decreased the association of CENP-C with cenDNA. CENP-C ChIP followed by qPCR analysis of cenDNA in KD-CCTT or

KD-CENP-A HeLa cells. *p < 0.05 (mean ± SD, n = 3 per group).

(E) CCTT knockdown by ASO treatment (ASO-CCTT #1 and #2) for 48 hours in HeLa cells. Quantification of CCTT level by qRT-PCR. **p < 0.01 (mean ± SD, n = 3 per group).

(F) CENP-A (white) IF analyses of HeLa cells that were transfected with negative control ASO (ASO-Ctrl) or two CCTT ASOs (ASO-CCTT #1 and #2) for 48 hours (top) and 96 hours (bottom). The nuclei stained by DAPI are outlined with dotted circles. Scale bar, 5 μm (left). The quantifications of CENP-A signals by IMARIS (right) are shown. n = 32 for Ctrl cells, n = 32 for ASO #1 cells, n = 33 for ASO #2 cells (top) and n = 33 for Ctrl cells, n = 30 for ASO #1 cells, n = 32 for ASO #2 cells (bottom). ***p < 0.001; ns, no significant difference (mean ± SD of three biological replicates).

(G) CENP-A (red) and CREST (green) IF analyses of $CCTT^{+/+}$ and $CCTT^{-/-}$ cells (left) and the quantification of CENP-A signals by IMARIS (right) are shown. n = 60 for both $CCTT^{+/+}$ and $CCTT^{-/-}$ cells. ns, no significant difference (mean ± SD of three biological replicates). Scale bar, 5 μm.

(H) CENP-A did not interact with CCTT. CENP-A RIP followed by qPCR analysis of CCTT in HeLa cells. IgG served as a negative control. ns, no significant difference (mean ± SD, n = 3 per group).

(I-J) The strategy to determine the BTP block efficiency (I). $CENP\text{-}C^{SNAP}$ detected by TMR-star staining (white) in HeLa cells. Scale bar, 10 μm (J).

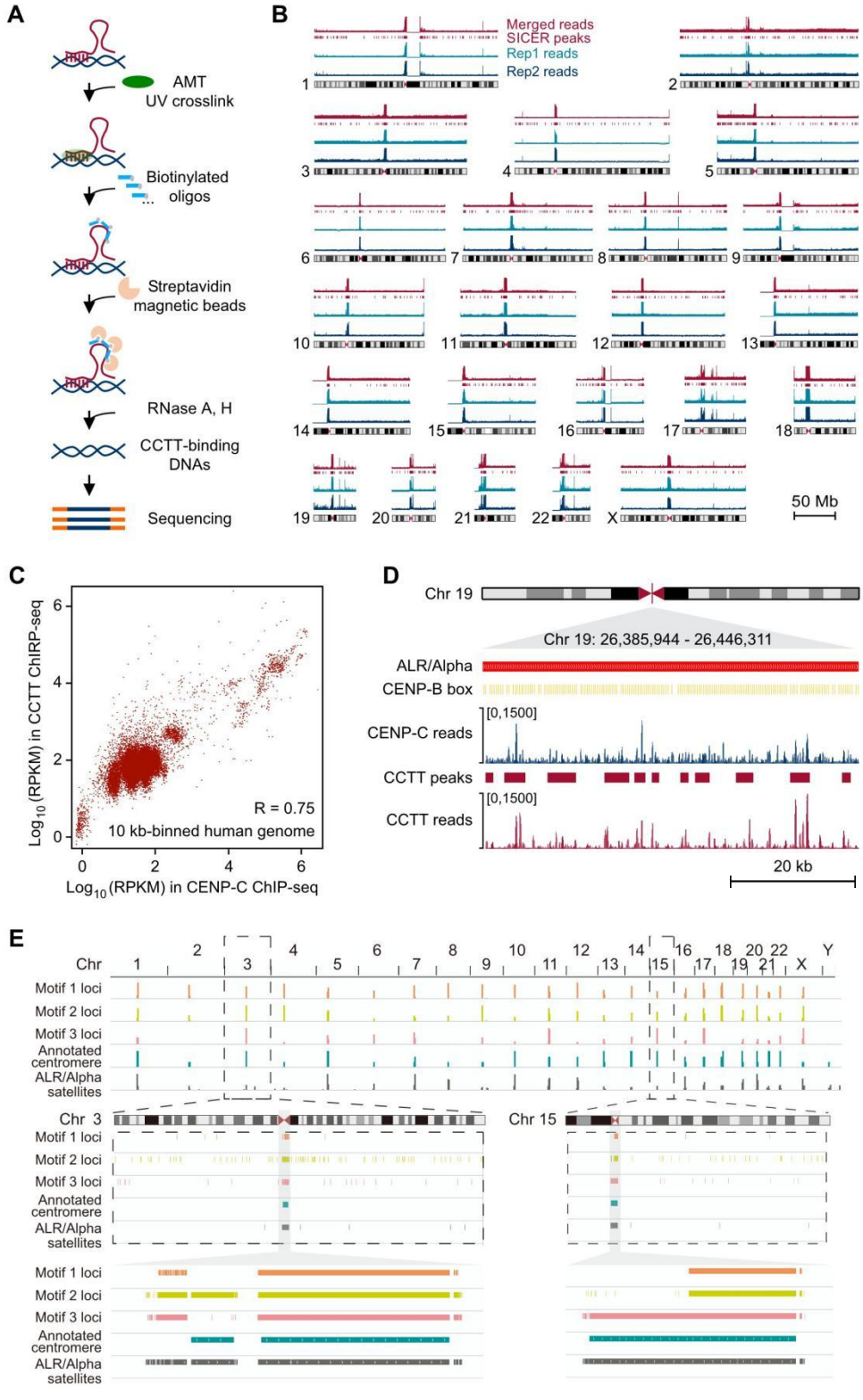

105 **Figure S4. CCTT Binds to CenDNA, Related to Figures 3 and 4**

106 (A) Strategy for CCTT ChIRP-seq with the crosslinker

4’-aminomethyltrioxsalen (AMT-ChIRP-seq) in HeLa cells.

(B) CCTT AMT-ChIRP-seq raw mapping data (repeat 1, repeat 2, and the merged one) as well as peaks identified by SICER for all chromosomes of HeLa cells.

(C) Correlation between CCTT and CENP-C binding signals in the 10 kb-binned human genome. Bins are shown as red dots. All R-values were calculated using Pearson correlation coefficient analysis.

(D) Typical genomic regions of Chr. 19 displaying CCTT and CENP-C binding signals at the centromere. Signals were normalized to RPKM.

(E) Using FIMO to map the top three CCTT-binding motifs to the whole genome with a cut-off p-value 1 x 10^{-7} (top). Typical genomic regions of Chr. 3 and Chr. 15 displaying three motifs binding signals on the whole chromosomes (middle) and at centromeres (bottom) are shown.

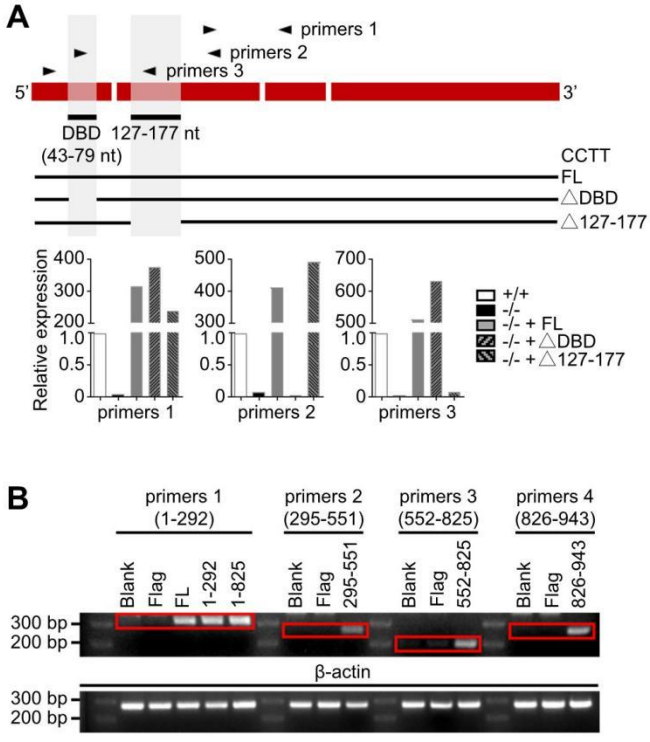

120 **Figure S5. Expressions of Mutant CCTT and CENP-C, Related to Figure 5**

121 (A) Quantification of full-length and mutant CCTT expressions in HeLa cells by
122 qRT-PCR. As shown in the diagram (top), primers 1 can detect the full-length
123 and mutant CCTT (bottom left), while primers 2 cannot detect ΔDBD CCTT
124 (bottom middle), and primers 3 cannot detect Δ127-177 CCTT (bottom right).
125 (B) Quantification of flag-tagged full-length and truncate CENP-C expressions
126 in HeLa cells by RT-PCR. RNA was treated by DNase I to rule out the possible
127 effects of the vector template DNA. Primers 1 can detect the full-length, 1-292,
128 and 1-855 CENP-C, while primers 2 can detect 296-551 CENP-C, primers 3
129 can detect 552-855 CENP-C, and primers 4 can detect 856-943 CENP-C
130 (shown in red boxes). β-actin was used as a loading control.

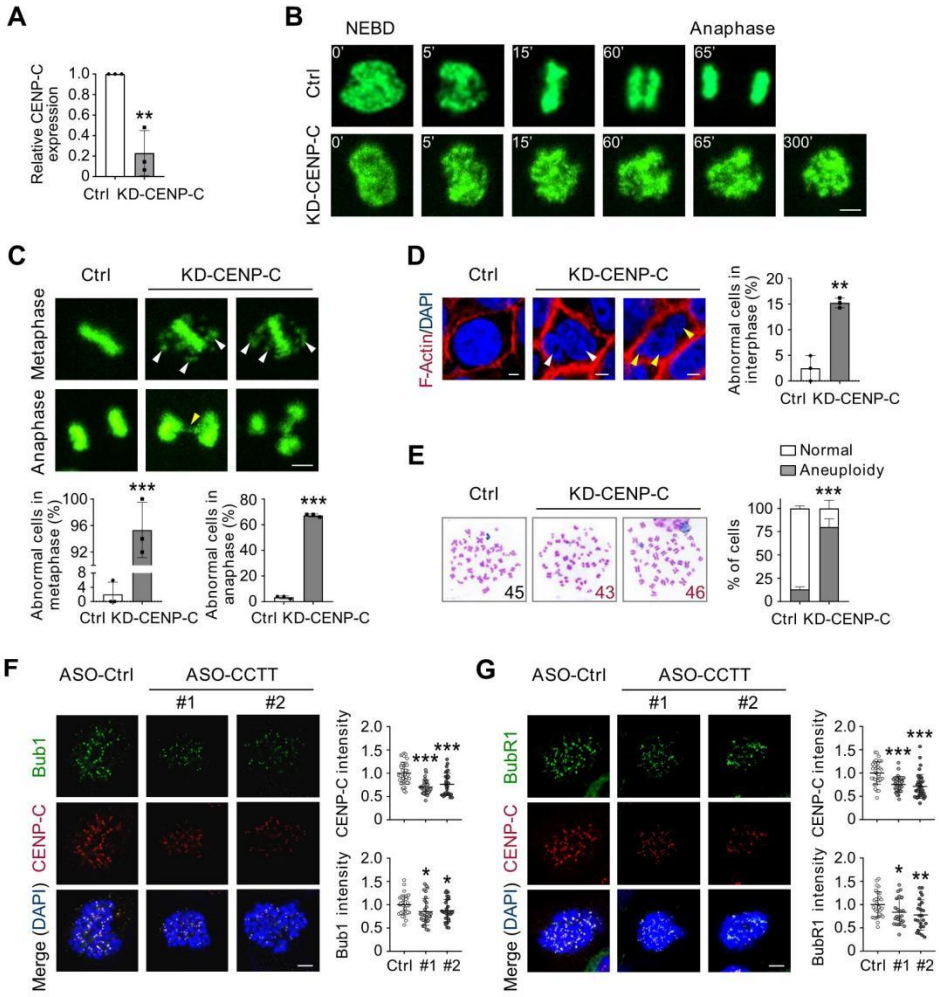

131 **Figure S6. CENP-C Is Required for Accurate Mitosis and Loss of CCTT**
132 **Impairs the Spindle Assembly Checkpoint, Related to Figure 6**

133 (A) Quantification of CENP-C expression by qRT-PCR in CENP-C knockdown
134 (KD-CENP-C) HeLa cells. **p < 0.01 (mean ± SD, n = 3 per group).

135 (B) KD-CENP-C HeLa cells exhibit prolonged mitosis. Representative
136 time-lapse microscopic images of Ctrl and KD-CENP-C HeLa cells expressing
137 histone H2B-GFP during mitosis are shown. Scale bar, 5 μm.

138 (C) KD-CENP-C caused mitotic errors in metaphase and anaphase HeLa cells.
139 Top: Representative images of mitotic errors by time-lapse assay, including
140 alignment defects (white arrowheads), chromosome bridges (yellow
141 arrowheads), and multipolar spindles. Bottom: Quantification of the
142 percentage of abnormal cells in metaphase (left) and anaphase (right). n =

150 for both Ctrl and KD-CENP-C. ***p < 0.001 (mean ± SD of three biological replicates). Scale bar, 5 μm.

(D) KD-CENP-C induced abnormal nuclei in interphase HeLa cells. Left: Binuclei (white arrowheads) and micronuclei (yellow arrowheads) were detected. Cells were stained with F-Actin (red) and DAPI (blue). Right: Quantification of the percentage of abnormal cells. n = 81 for Ctrl, n = 105 for KD-CENP-C. **p < 0.01 (mean ± SD of three biological replicates). Scale bars, 5 μm.

(E) KD-CENP-C caused aneuploidy in HCT116 cells. Left: Representative images of chromosomes and abnormal numbers are highlighted in red. Right: Quantification of the percentage of aneuploid cells. n = 60 for both Ctrl and KD-CENP-C. ***p < 0.001 (mean ± SD of three biological replicates).

(F) Representative images of Bub1 (green) and CENP-C (red) IF analyses of CCTT knockdown HeLa cells in pro-metaphase (left). The signal intensities of Bub1 (n = 31 for ASO-Ctrl, n = 30 for ASO-CCTT #1, and n = 27 for ASO-CCTT #2) and CENP-C (n = 36 for ASO-Ctrl, n = 27 for ASO-CCTT #1, and n = 32 for ASO-CCTT #2) were quantified by IMARIS (right). *p < 0.05; ***p < 0.001 (mean ± SD of three biological replicates). Scale bar, 5 μm.

(G) Representative images of BubR1 (green) and CENP-C (red) IF analyses of CCTT knockdown HeLa cells in pro-metaphase (left). The signal intensities of BubR1 (n = 29 for ASO-Ctrl, n = 23 for ASO-CCTT #1, and n = 24 for ASO-CCTT #2) and CENP-C (n = 34 for ASO-Ctrl, n = 33 for ASO-CCTT #1, and n = 38 for ASO-CCTT #2) were quantified by IMARIS (right). *p < 0.05; **p < 0.01; ***p < 0.001 (mean ± SD of three biological replicates). Scale bar, 5 μm.

Table S2. CCTT ORFs of *In Vitro* Translation Assay, Related to Star Methods

CCTT ORF1 CDS

ATGCAGCTCCCCTTCCCTCCCATTCCACCATCCACTGTCCCCAGCAAGA
ACCTGCGGGAGGGTGGCCCAATGGGGAGAAAACTAAGGATTCGGTGTT
GGGACCACTCCTGCCCTGACCTGCCCTGTGACTCCGTCATACTCTCCAA
AGGCCAGACCCTCCTAGACCAGCTGGAACCACCATCAAGATGTCCCCA
GCCATGTCAGACTCTGGGGCCCCAGGCGGAGGGCAACCAGATGTCTTC
AGCTCCAAGTCTGGCCTCTCCTCCCAGCAAGCAGCCAACTGCAGAGAC
CTTGGAAAGGATCAACCATATACAATGTCCATTTCCTGCCCTCTAA

CCTT ORF2 CDS

ATGTCCCCAGCCATGTCAGACTCTGGGGCCCCAGGCGGAGGGCAACCA
GATGTCTTCAGCTCCAAGTCTGGCCTCTCCTCCCAGCAAGCAGCCAACT
GCAGAGACCTTGGAAAGGATCAACCATATACAATGTCCATTTCCTGCCC
TCTAACCTGGCAGGGGAGCAAGGCCCAGCCAAGGAGTTACAGAAACTG
A